Supplementary Materials for

Multiple C-C bond formation upon electrocatalytic reduction of CO_2 by an iron-based molecular macrocycle

Si-Thanh Dong, Chen Xu and Benedikt Lassalle-Kaiser.*

Correspondence to: benedikt.lassalle@synchrotron-soleil.fr

This PDF file includes:

Materials and Methods
- Electrochemical flow cell design and fabrication
- Catalyst ink and electrodes preparation
- Electrocatalytic experiments
- Gas chromatography and NMR characterization
- Faradaic efficiency calculation
- Isotopic labeling experiments
- Electrode potential conversion
- Infrared (IR) spectroscopy experiments
- X-ray absorption spectroscopy experiments
- ICP-MS experiments

Supplementary Text: Finite element method modeling and results
Figs. S1 to S13
Tables S1 to S4
References (*1–11*)

Materials and Methods

Electrochemical flow cell design and fabrication

The electrochemical cell design is inspired by the work of Ager and co-workers.[1] It is 3D printed using the Objet30 Pro Polyjet 3D printer (Stratasys), with VeroClear materials and SUP706 support materials. The flow channels in both cathodic and anodic sides are similar, with dimensions of 15 x 5 x 2.5 mm^3. The inlet and outlet of the cell are made by gluing PEEK tubing (ID 0.75 mm, OD 1/16 inch) to the designated hole with Torr-seal epoxy. The cell is thoroughly cleaned and sonicated in a diluted solution of NaOH (~2%) after printing to remove the support material and sonicated in water purified by reverse osmosis to 18 MΩ before each experiment to remove any possible contaminants.

Catalyst ink and electrodes preparation

8 mg of carbon black (Vulcan XC72 – Fuel Cell Store) are dispersed in 6 mL of dimethylformamide (DMF – 99.8% – VWR) by sonicating the mixture for 30 minutes at high power (FB11209 Fischer brand sonicator). 0.74 mg of FePc (Porphychem) dissolved into 2 mL of DMF is added to the carbon black dispersion, and the mixture is then sonicated for 10 minutes at low power. 80 µL of Nafion D-520 solution (Alfa Aesar) is then added, with another 10 minutes of sonication at low power.

The working electrodes are cast right after the ink is made to avoid the aggregation of carbon black. A glassy carbon plate (HTW) with the dimension of 25 x 10 x 0.3 mm^3 is kept on a hotplate at 80°C. A 70 µL drop of ink is cast onto the glassy carbon plate, covering the whole surface of the electrode. The total volume cast on one electrode is 1167 µL, yielding a surface concentration of the catalyst around 80 $nmol/cm^2$. After the addition of the ink, the electrode is kept in a vacuum desiccator at 80°C overnight to fully evaporate the DMF solvent.

A nickel plate (99.9% trace metal basis, Sigma-Aldrich) with the dimension of 25 x 10 x 0.5 mm^3 is used as the counter electrode. The electrode is polished gradually with 9 µm, 6 µm, and 3 µm liquid diamond suspensions (Bio DIAMANT®) and repolished with 3 µm liquid diamond suspension after each electrolysis experiment.

An LF-1 leak free 3.4 M Ag/AgCl reference electrode from Innovative Instruments is used as the reference electrode in all experiments. It is kept in a 0.05 M solution of H_2SO_4 and is thoroughly washed before and after each experiment with water purified by reverse osmosis to 18 MΩ.

Electrocatalytic experiments

The assembly of the electrochemical cell is shown in Figure 1. The four layers are pressed tightly together by four M3 bolts. The reference electrode is held in place with a 3D-printed piece, an O-ring, and two M3 bolts. The setup of the electrolysis system is shown in Figure S2. 25 mL of 0.1 M $KHCO_3$ (VWR) solution is added to each catholyte and anolyte container. The headspace volume of the catholyte container is derived by the mass difference of water between a fully filled versus a 25-mL-filled container, yielding 9.1 mL. Before an experiment, the catholyte solution is bubbled with CO_2 (Alphagaz 1 – Air

Liquide), Ar (Alphagaz 2 – Air Liquide), or CO (Air Liquide) for at least 15 minutes while a peristaltic pump circulates the solution through the whole system. For the control experiments with alternative substrates, a 30 mM solution of HCHO (methanol-free, Thermo Scientific) in 0.1 M $KCHO_3$ is prepared beforehand and purged with Ar or CO_2, similar to the description above. The flow rate of the Ismatec peristaltic pump is 1 mL/min, and the pump is calibrated before each experiment using a 5-mL volumetric flask.

Gas chromatography and NMR characterization

A 2-module Micro GC FUSION® Gas analyzer is used to characterize gaseous products in this study. Module A has a 10-meter Rt-Molsieve 5A column, while module B has a 12-meter Rt-Q-bond column. Both modules use thermal conductivity detectors. The parameters of each module are shown in table 1.

Table S1. Gas chromatography method parameters

Parameters	Module A	Module B
Carrier gas	Argon	Helium
Column temperature	55°C (hold 20s) to 100°C (hold 185s), ramp rate 1°C/s	50°C (hold 50s) to 100°C (hold 100s), ramp rate 1°C/s
Backflush time	10.9s	N/A
Column pressure	20 psi	17 psi
Inlet temperature	50°C	50°C
Detector temperature	70°C	70°C
Sample pump time	10s	10 s
Injector temperature	70°C	90°C
Inject time	120 ms	90 ms

The gas chromatograph is calibrated using mixtures of gases with known concentrations. A 2.9% (v/v) mixture of H_2 in Ar and a 0.5% (v/v) mixture of CO in He from Air Liquide are used to calibrate CO and H_2. For CH_4, C_2H_4, C_2H_6, C_3H_6, C_3H_8, a mixture of 100 ppm (v/v) of each gases in N_2 from Air Products is used. For n-C_4H_{10}, a pure sample of the gas from Messer is used. A linear forced-through zero regression is performed to establish the relationship between the peak area and the volume concentration for each gas product, as recommended by the manufacturer of the chromatograph. The peak corresponding to pentane (C_5H_{12}) was identified by sampling the headspace of a flask containing liquid pentane. However, it was not calibrated due to the difficulties regarding the calibration of volatile liquid organic products with gas chromatograph in the low concentration region observed in our experiments.

NMR measurement is used to detect liquid products that may be present in the electrolyte. An aliquot of catholyte is sampled after each electrolysis. A solution of 50 mM Phenol and 10 mM DMSO in D_2O is used as standards for the NMR measurement. 450 µL of the catholyte solution and 50 µL of the standard solution are thoroughly mixed and dropped

into an NMR tube for measurement. A 400 MHz Bruker NMR spectrometer with a water suppression program is used for the measurement.

Faradaic efficiency calculation

A gas chromatograph measurement is performed every 30 minutes in the course of the 2-hour electrolysis. The volume percentages of each gas are derived from the calibration line obtained from the procedure described above. The mole numbers of each product are calculated using the ideal gas law:

$$n = \frac{P \times (\%V \times V)}{R \times T}$$

where P, V, and T are the headspace pressure, volume, and temperature, of the catholyte container, respectively. %V is the volume percentage measured by the gas chromatograph, and R is the gas constant (8.314 $J.mol^{-1}.K^{-1}$). Due to the low amount of generated products compared to the headspace volume, as well as the climate-controlled condition of the laboratory, the values of the pressure and the temperature in the headspace are assumed to be the values of atmospheric pressure (1.013 hPa) and room temperature (298 K).

The Faradaic efficiency of all gaseous products is then calculated using the formula:

$$\%FE = \frac{n \times e \times F}{Q}$$

where n is the mole number of the corresponding products, e is the number of electrons needed to reduce CO_2 (or H_2O in the case of H_2) to that product, F is the Faraday constant (96490 $C.mol^{-1}$) and Q (C) is the total charge passed through the system, given by the potentiostat.

The procedure for calculating the Faradaic efficiency of liquid products is similar, except that the calculation of the mole number is done directly using the molar concentration measured by NMR with a DMSO internal standard.

Isotopic labeling experiments

The Micro GC FUSION® is coupled to the Omni Star GSD 320, O2 mass spectrometer by connecting the analytical outlet of module B of the gas chromatograph to the capillary of the mass spectrometer. A multiple ion detection mode with an SEM detector is used to monitor the masses of the theoretical fragments of C_2 to C_4 products based on the NIST database.[2] The parameters of the detection method are summarized in Table S2.

Table S2. Mass spectrometry method parameters

Parameters	Value
Inlet temperature	120°C
Capillary temperature	150°C
Dwell time	200 ms
SEM voltage	900 V
Resolution	50
Pause calibrate	1.00

A standard electrocatalytic experiment with $^{12}CO_2$ is performed as described in section 3. The mass spectrometer measurement is started simultaneously with the gas chromatograph

measurement every 30 minutes during the 2-hour electrolysis. For the labeling experiment, 99.9% $^{13}CO_2$ from Eurisotop is purged in the catholyte container for 15 minutes.

The major fragment of ^{12}CO in a mass spectrum is at m/z = 28, overlapping with major fragments of ethane, ethylene, and propane. Since the dominant product of the electrochemical reduction of CO_2 in our system is CO and the amount of C_{2+} products detected is orders of magnitude lower, although the gas chromatograph can separate CO and C_{2+} products somewhat effectively, the background signal from CO fragment is too large to detect any mass signals of C_{2+} products with masses in the vicinity of m/z = 28. Similarly, the major fragment of $^{12}CO_2$ at m/z = 44 overlaps with the main fragments of C_3 and C_4 products. As the catholyte is saturated with CO_2, it results in a high background signal around C_3 and C_4 products' main fragments near m/z = 44, making the detection of these fragments challenging. However, as shown in Figure S4, signals of the fragment with m/z = 41 (C_3H_5) are detected when $^{12}CO_2$ is used and disappear when the substrate is changed to $^{13}CO_2$. Since the m/z region of C_4 products (m/z = 56) is free of any species that could present high background signal, they are chosen to be the main focus in our isotopic labeling experiments, as shown in Fig. 2C and D in the main text.

Electrode potential conversion

The conversion of potential from 3.4 M Ag/AgCl reference electrode to reversible hydrogen electrode is performed using the formula:

$E_{RHE} = E_{Ag/AgCl} + 0.205\ V + 0.0591 \times pH$

where the pH of 0.1 M $KHCO_3$ is 6.8 when saturated with CO_2 and 8.5 when saturated with Ar; the pH of 0.1 M KCl is 6.3 when saturated with Ar. All potential values are rounded to the first decimal place.

Infrared (IR) spectroscopy experiments

The infrared measurements were performed at the AILES beamline[3] of Synchrotron SOLEIL. The beamline is equipped with a Fourier Transform infrared spectrometer (IFS 125 from Bruker Instruments) working under vacuum (10^{-4} mbar). The spectra are recorded using a Globar source, a KBr beamsplitter, and a homemade MCT detector cooled at 4.2K.[4] Two different set-ups were used for this study. References samples (pure powder) were analyzed by using ATR (Attenuated Total Reflectance) technique [4] with a single reflection on a 2mm diamond crystal. Modified-electrode samples were analyzed by using an optical setup (A513-Bruker), allowing reflectivity measurement at grazing angle (70°), the spectrum of the glassy carbon modified with catalyst-free ink being used as a reference.

X-ray absorption spectroscopy experiments

XAS experiments were performed on the LUCIA[5] of Synchrotron SOLEIL, with a ring current of 500 mA and a nominal energy of 2.3 GeV. On LUCIA, The beamline energy was selected by means of a Si (111) double-crystal monochromator, and the beam size was 2 x 2 mm^2. The electrocatalytic flow cell was placed in the experimental chamber under vacuum, with a 25° outgoing angle with respect to the detector, which is located at a 90° angle from the incident beam path. The experimental setup is similar to the one described

in Section 4.3. However, a silver wire glued in the cell was used as the pseudo reference electrode since the mini Ag/AgCl reference electrode is not vacuum-compatible. In addition, the gas is kept bubbling during the whole measurement, as the gas products were not characterized during the spectro-electrochemical measurement. XANES data were collected as fluorescence excitation spectra using an SDD Bruker detector. The reference spectra of FePc, Fe metal, and $Fe_3O_4$are measured with 6-mm round pellets containing 1 mg of sample and 40 mg of graphite window materials,. All XAS data were normalized to the intensity of the incoming beam and reduced using the Athena software.[6]

ICP-MS experiments

Table S3 - S6 show the amount of metal and inorganic contaminants present in FePc and H_2Pc powders (LOD stands for limit of detection). The ICP-MS analysis were performed by ROC Analyse (https://sarm.cnrs.fr/index.html/), a laboratory of CNRS, with 200 mg of FePc and H_2Pc powder.

Table S3. Metallic components of phthalocyanine (H_2Pc)

Metal	Value (µg/g)	Limit of detection (µg/g)	Maximum error (%)
Co	< LOD	0.08	25
Cr	< LOD	0.5	25
Cu	< LOD	2	25
Ni	< LOD	2	25
Sb	13.6	0.06	5
Sn	< LOD	0.3	25
V	< LOD	0.85	25
Zn	< LOD	7.0	25

Table S4. Inorganic components of phthalocyanine (H_2Pc)

Inorganic species	Value (%w)	Limit of detection (%w)	Maximum error (%)
SiO_2	1.04	0.05	10
Fe_2O_3	< LOD	0.015	2
MnO	< LOD	0.015	25
MgO	< LOD	0.03	25

Table S5. Metallic components of iron phthalocyanine (FePc)

Metal	Value (µg/g)	Limit of detection (µg/g)	Maximum error (%)
Co	12.2	0.08	10
Cr	1.4	0.5	10
Cu	2	2	25
Ni	8	2	25
Sb	14.3	0.06	5
Sn	< LOD	0.004	20
V	9.5	0.85	15
Zn	11.6	7.0	20

Table S6. Inorganic components of iron phthalocyanine (FePc)

Inorganic species	Value (%w)	Limit of detection (%w)	Maximum error (%)
SiO_2	< LOD	0.05	25
Fe_2O_3	19.76	0.015	2
MnO	< LOD	0.015	25
MgO	< LOD	0.03	25

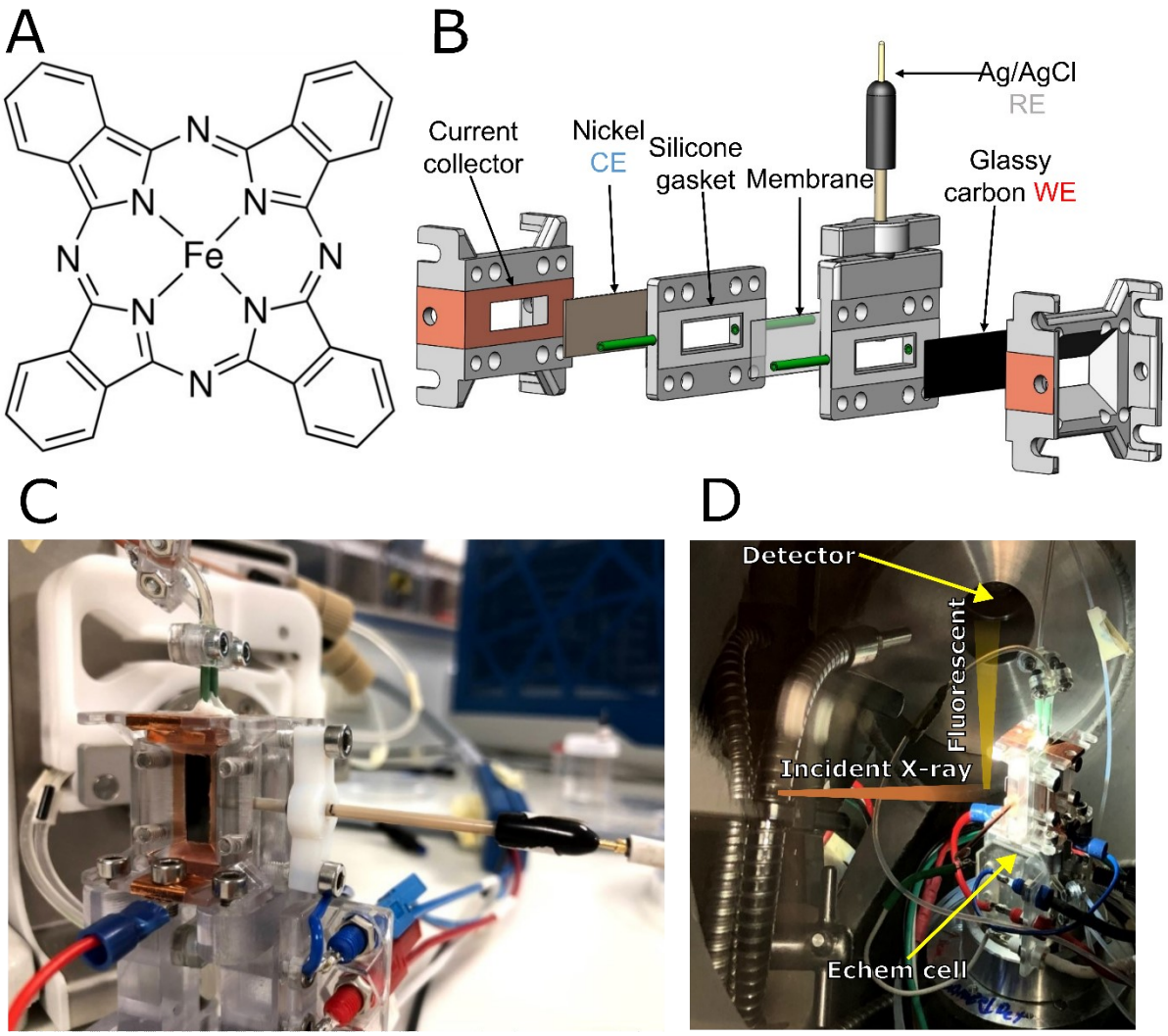

Fig. S1.

(A) FePc structure; **(B)** Exploded view of the electrocatalytic flow cell in which the electrocatalytic experiments were performed **(C)** Picture of the electrochemical flow reactor in a standard experiment **(D)** and in the experimental chamber of the LUCIA beamline at Synchrotron SOLEIL in an X-ray spectroelectrochemical experiment.

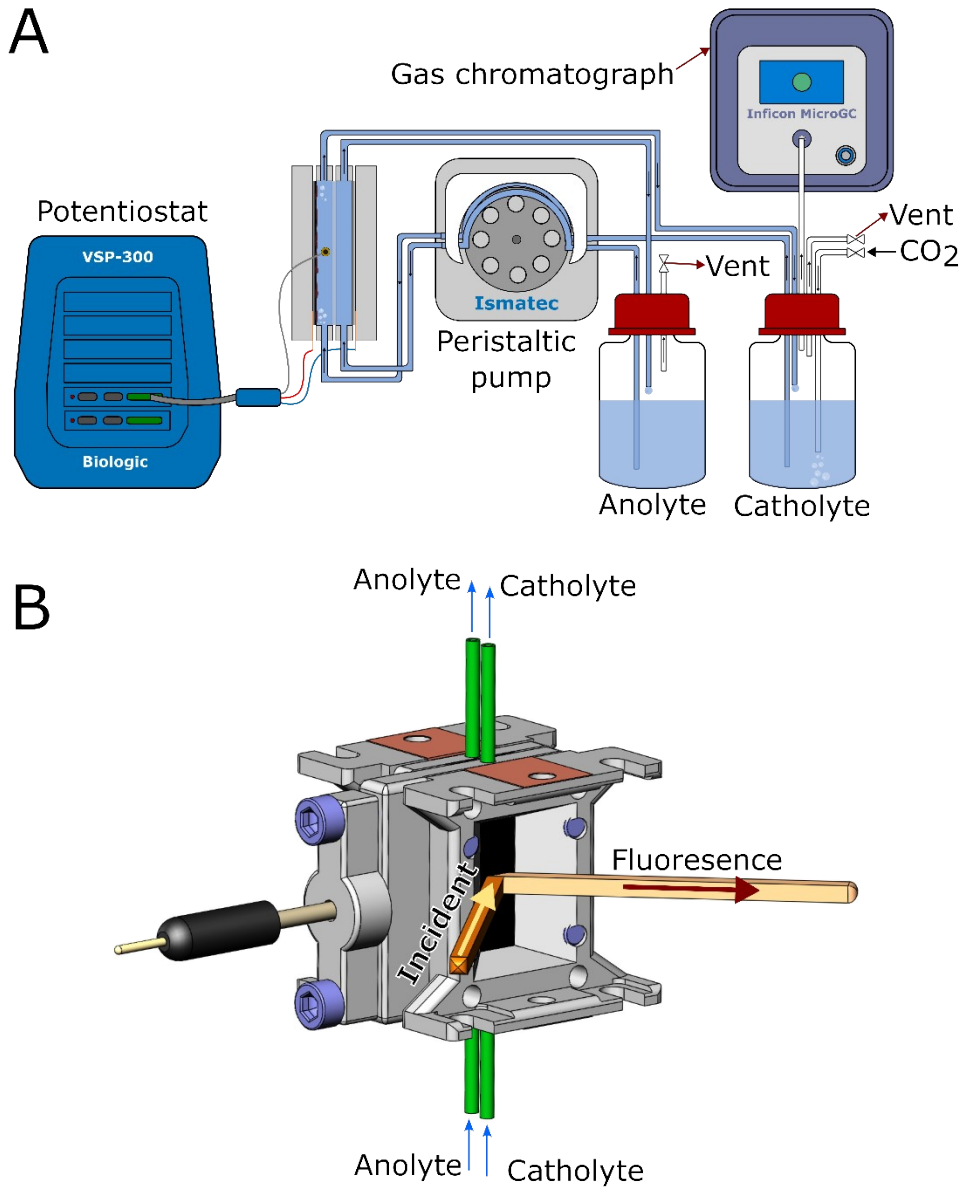

Fig. S2.

(A) Simplified scheme of the standard experimental setup used in this study. **(B)** The X-ray spectroelectrochemical cell with a scheme showing the beam path

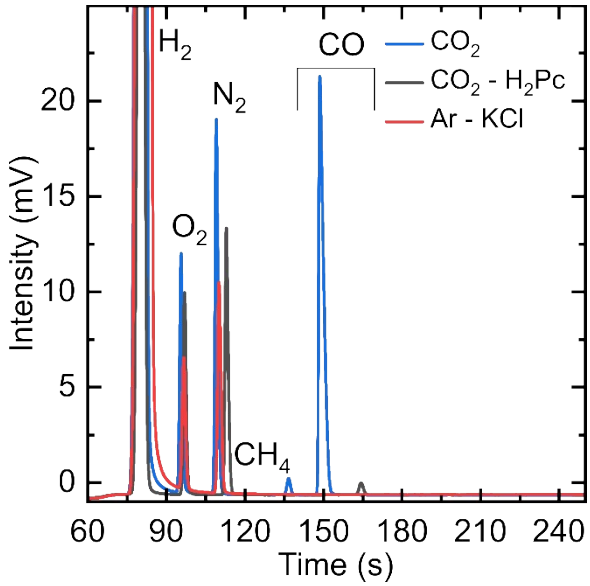

Fig. S3.

Gas chromatograms of Module A after 2-hour electrolysis at -1.1 V *vs.* RHE with FePc-modified electrodes under Ar (red) or CO_2 (blue) and with an H_2Pc-modified electrode under CO_2 (black)

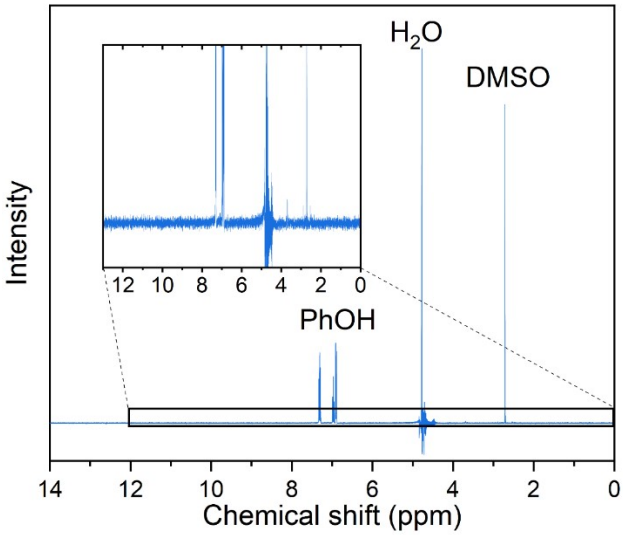

Fig. S4.

^{1}H NMR spectra of catholyte after 2-hour electrolysis in CO_2 saturated electrolyte at -1.1 V *vs.* RHE with FePc catalyst. The signal from PhOH and DMSO are from internal references of the sample.

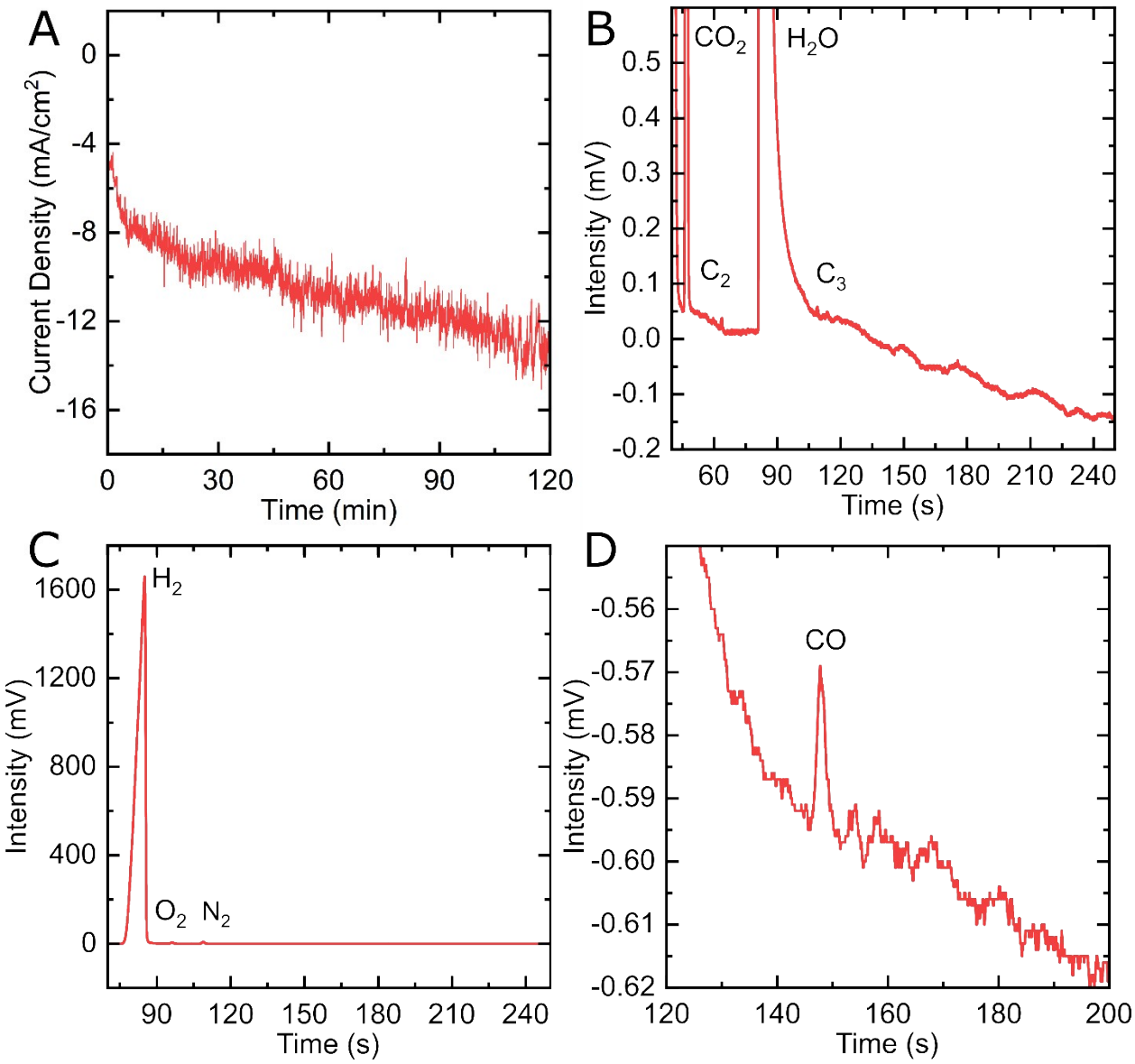

Fig. S5

(A) Chronoamperometric curves, **(B)** Module B gas chromatograms, **(C)** Module A gas chromatograms – zoomed, and **(D)** Module A gas chromatogram of FePc-modified electrodes under Ar in 0.1 M $KHCO_3$. Chronoamperometric experiments are performed at –1.7 V vs. Ag/AgCl for two hours, after which a GC samples the resulting gaseous products.

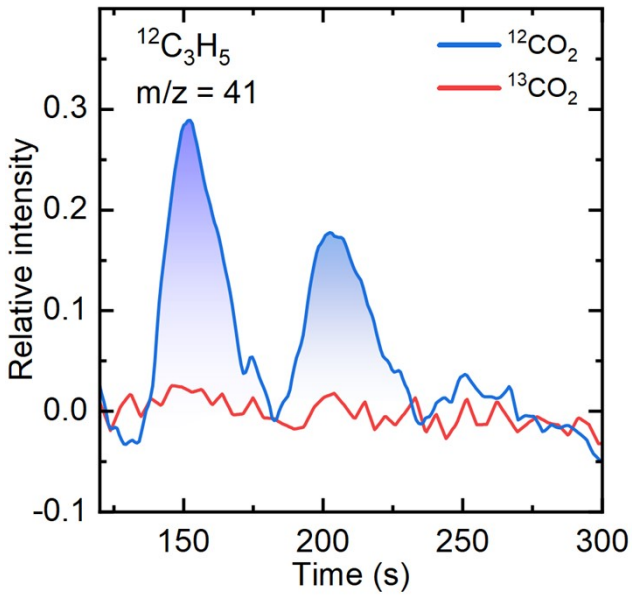

Fig. S6.

GC-MS chromatogram of mass m/z = 41 of $^{12}C_3H_5$ at the region of the retention time of C_3 (dark blue, t = 135-165 s) and C_4 (light blue, t = 190-220 s) products. C_3H_5 is a major fragment in the mass spectrum of C_4H_{10}[7] and C_4H_8.[8] Chronoamperometric experiments were performed on FePc-modified electrodes at –1.1 V vs. RHE for two hours, after which the GC-MS sampled the resulting gaseous products. The chromatograms were averaged from three independent experiments.

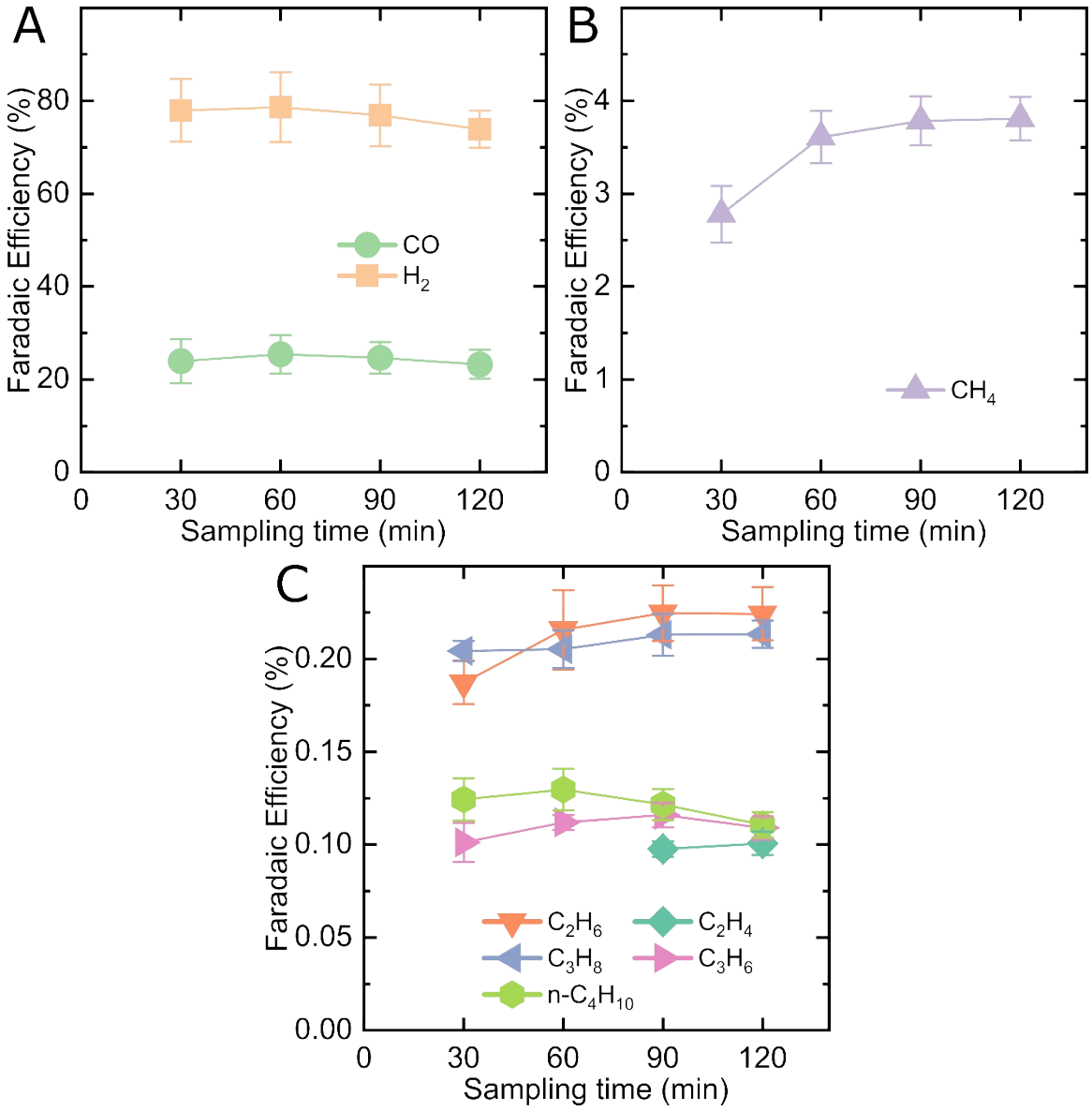

Fig. S7

Evolution of Faradaic efficiencies for the obtained CO and H_2 **(A)**, CH_4 **(B)**, and C_{2+} products **(C)** during 2-hour electrolysis with FePc-modified electrodes at -1.1 V vs. RHE under CO_2-saturated $KHCO_3$ electrolyte. The value of methane and ethylene at 30 and 60 minutes are outliers: The amount of CH_4 exists at 30 and 60 minutes is close to the detection limit of the gas chromatograph's module A, resulting in higher uncertainty. For ethylene, the CO_2 peak partially overlaps with the peak of ethylene, thus the small amounts of C_2H_4 after 30 and 60 minutes of electrolysis were not visible.

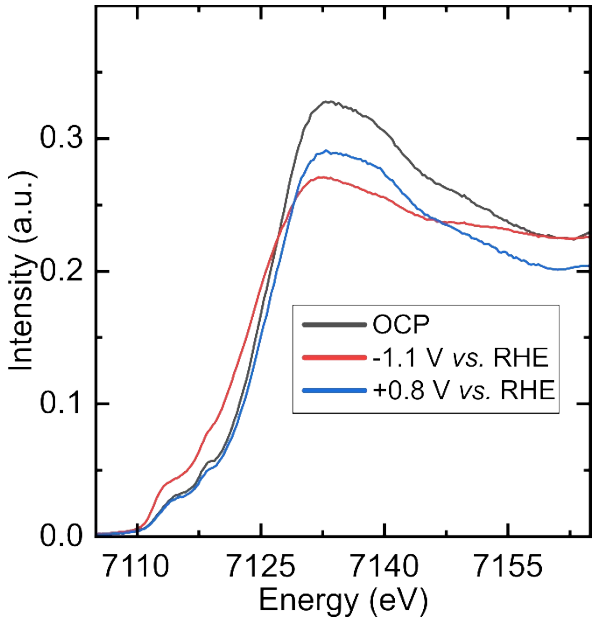

Fig. S8.

In situ and *operando* X-ray absorption raw (un-normalized) spectra collected on an FePc-modified electrode under different conditions**.** The spectra correspond to an FePc-modified electrode under a CO_2 atmosphere poised at OCP (black), at -1.1 V *vs.* RHE (red), and going back at +0.8 V *vs.* RHE (blue). The total time of the experiment is approximately 4.5 hours, with constant electrolyte flow at 1 mL/min. The decrease in intensity accounts for *ca.* 10% material loss.

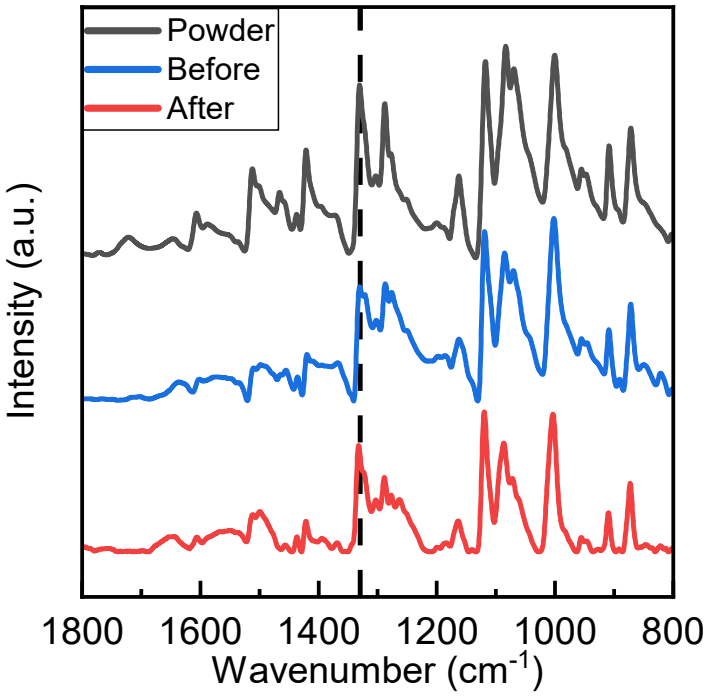

Fig. S9.

IR spectra of the FePc catalyst powder and of FePc-modified electrodes before and after 2-hours electrolysis at -1.1 V *vs.* RHE. Characteristic vibrational peaks of the phthalocyanine ligand in a typical metal phthalocyanine species are: stretching modes of C=C, C–N=C, isoindole and pyrrole groups from 1800 to 1330 cm^{-1}; as well as scissoring modes of C–H and isoindole groups from 1330 cm^{-1} to 800 cm^{-1}.[9,10]

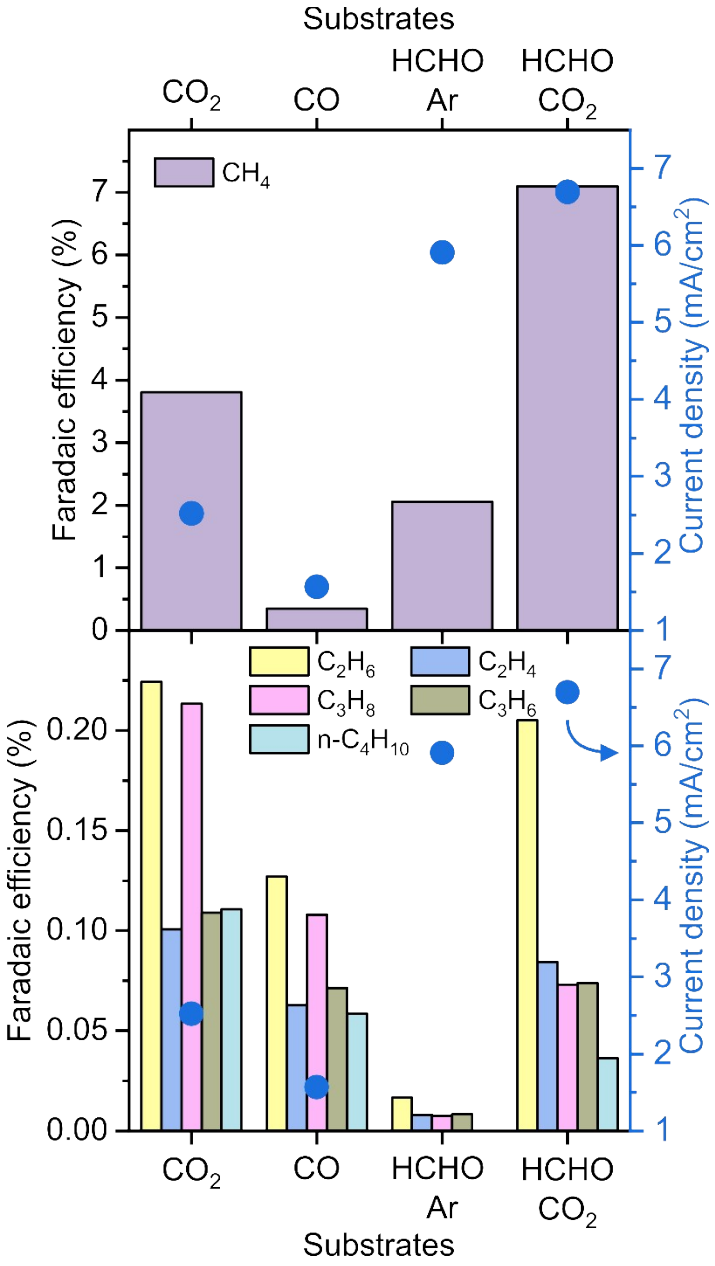

Fig. S10.

CH_4 and C_{2+} products distribution with faradaic efficiencies after 2-hour electrolysis at -1.7 V *vs.* Ag/AgCl with different substrates using an FePc-modified electrode.

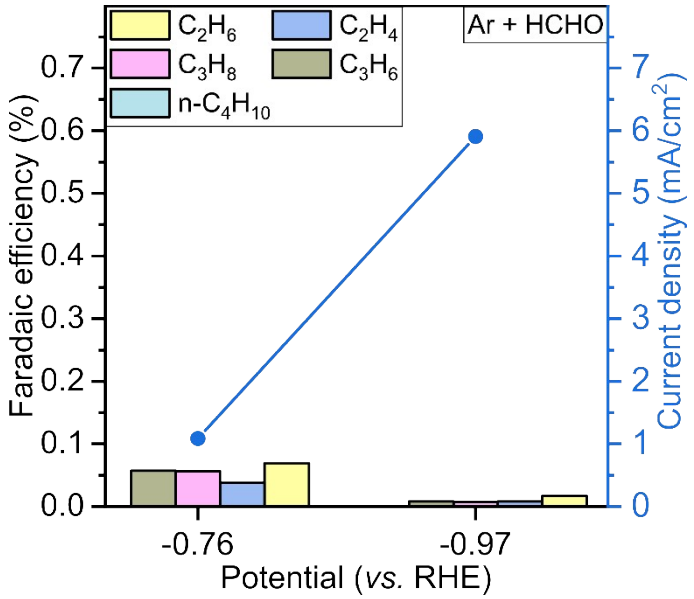

Fig. S11.

C_{2+} products faradaic efficiencies after 2-hour electrolysis at -0.76 V and -0.97 V *vs.* RHE (-1.7 V and -1.5 V *vs.* Ag/AgCl, respectively) with 30 mM HCHO under Ar atmosphere using an FePc-modified electrode.

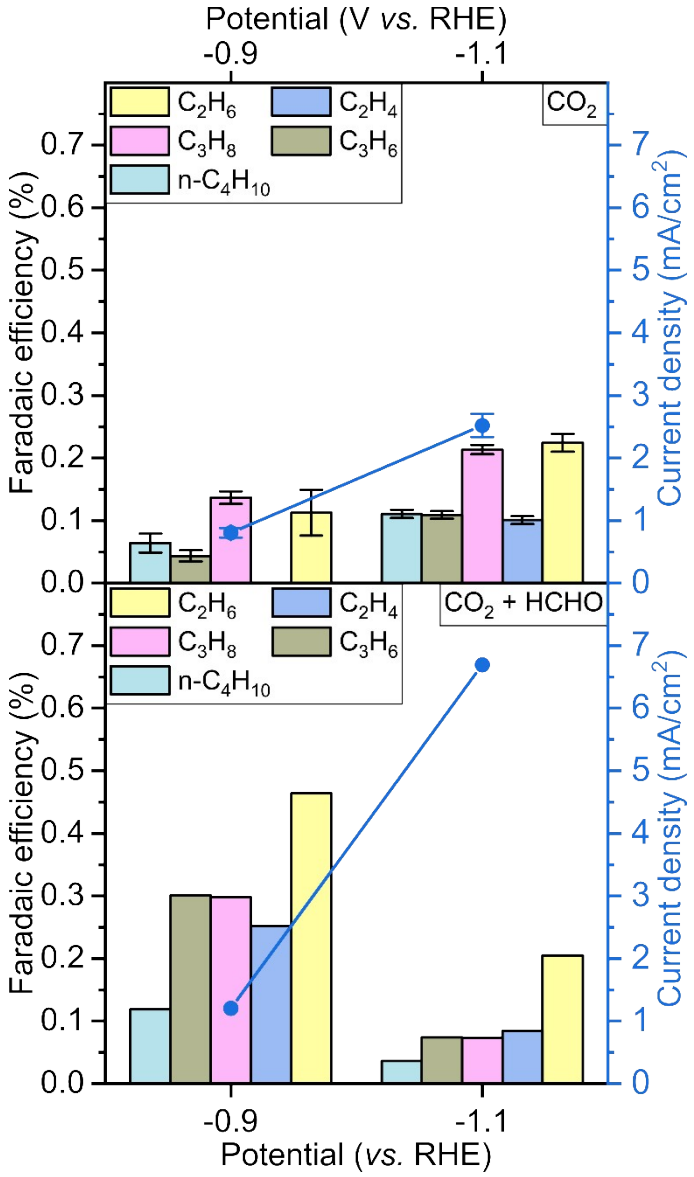

Fig. S12.

C_{2+} products faradaic efficiencies after 2-hour electrolysis at -0.9 V and -1.1 V *vs.* RHE (-1.7 V and -1.5 V *vs.* Ag/AgCl, respectively) under only CO_2 and CO_2 with 30 mM HCHO atmosphere using an FePc-modified electrode.

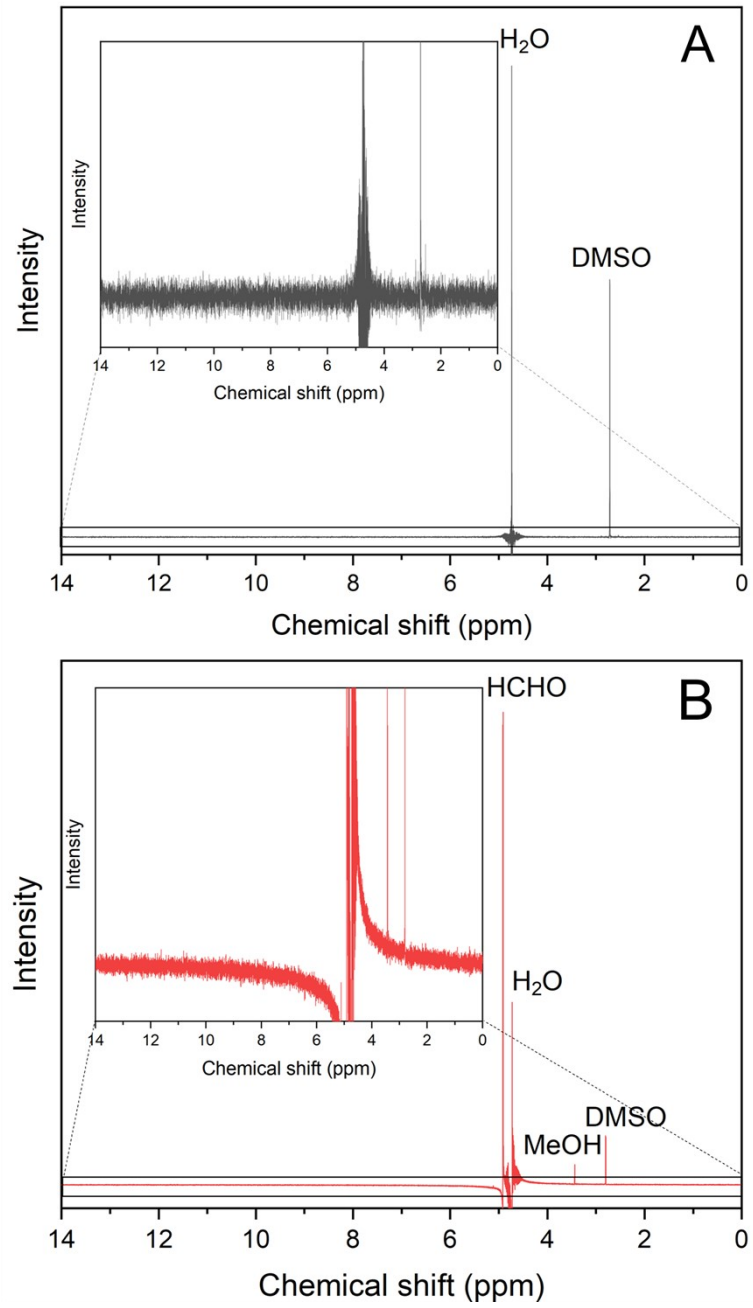

Fig. S13.

^{1}H NMR spectra of catholyte after 2-hour electrolysis in CO saturated electrolyte (A), Ar saturated electrolyte with 30 mM HCHO (B) at -0.97 V *vs.* RHE (-1.7 V *vs.* Ag/AgCl) with an FePc-modified electrode.

Supplementary Text: Finite element method modeling and results

Geometry of the flow cell: 2D model and meshing

A two-dimensional model of our electrochemical flow cell is built with the COMSOL software version 5.2. The model consists of the working electrode half of the cell, which is shown in Fig. S14a. Fig. S14b overlays the model on a picture of the actual electrochemical cell. *Table S3* summarizes the geometric parameters of the model. The distance from the working electrode to the Nafion membrane includes the thickness of the flow channel as well as the thickness of the two silicone gaskets between the electrode and the cell and between the membrane and the cell. The width of the channel is not used to build the model, but it is used to derive the active area of the electrode, which is described in more detail in the following section. The model is meshed automatically using Physics-control meshed sequence with *Finer* element size. The model after meshing is shown in Fig. S14c.

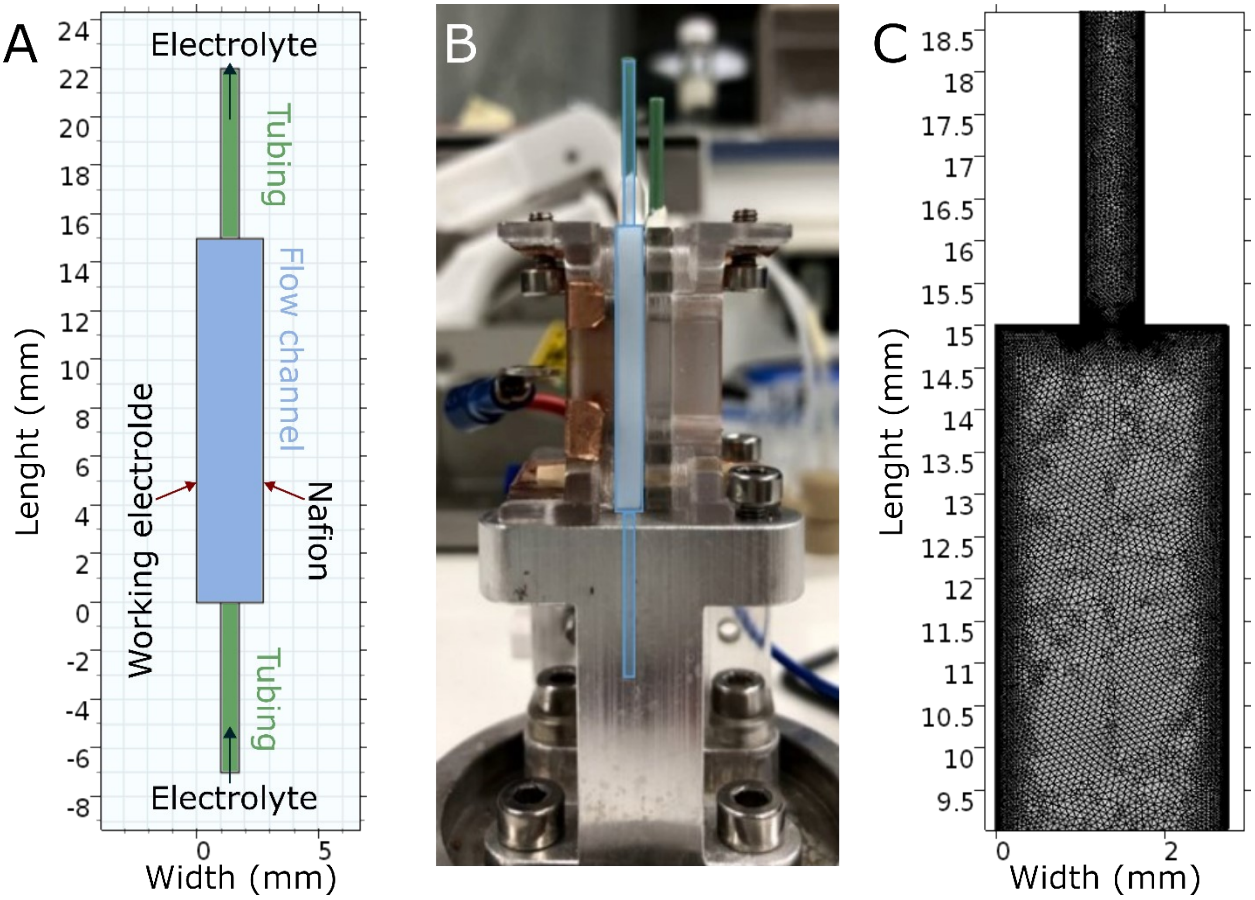

Fig. S14.
2D model of the electrochemical flow cell built in COMSOL 5.2 (a); Overlay of the model geometry on a real picture of the electrochemical flow cell (b); 2D model after meshing *(c)*

Table S7. Dimension parameters for modelling the electrochemical flow cell

Parameters	Value	Unit
Tubing radius	0.375	mm
Tubing length	7	mm
Flow channel width	5	mm
Flow channel length	15	mm
Flow channel thickness	2.5	mm
Gasket thickness	0.127	mm

Multiphysics: Laminar flow and transport of diluted species

We based the simulation of our electrochemical flow cell on the model established by Gatrell *et al.* [11] and Ager *et al.*[1]

To simulate the flow of the electrolyte in our cell, the laminar flow physics module is used. The Reynolds number associated with our electrochemical flow cell when an aqueous electrolyte is flown at 1 mL/min is calculated as follows:

$$Re = \frac{\rho \mu L}{u} = \frac{997\,\frac{kg}{m^3} \times 8.90 \times 10^{-4} Pa.s \times 3.6 \times 10^{-3} m}{1.21 \times 10^{-3} m/s} \approx 2.6$$

where ρ (kg/m^3) is the density of the fluid, μ (kg/(m.s)) is the dynamic viscosity of the fluid, L (m) is the characteristic linear dimension, and u (m/s) is the flow speed. For a rectangular channel, the hydraulic diameter is used as the characteristic linear dimension. Since the electrolyte is a diluted bicarbonate solution, we consider the density and dynamic viscosity of the electrolyte to be similar to that of water. Laminar flow occurs at Re < 2000; thus the Reynold number of our system indicates that the flow is strictly in the laminar regime.

The inlet boundary condition is applied to the bottom boundary of the bottom tubing. Normal inflow velocity mode is used, and the velocity of the fluid is calculated by dividing the flow rate by the cross-section area of the tubing. The outlet boundary condition is applied to the top boundary of the top tubing, with outlet pressure equal to zero, and the suppress backflow option is enabled. No slip boundary condition is applied to all other boundaries. Initial values of velocity and pressure across all domains are set to zero.

To calculate the consumption rate of CO_2 and the generation rate of CO, the transport of dilute species physics module is used. Two modes of mass transport are considered: diffusion and convection. The velocity field resulting from the laminar flow physics calculation is used in the model inputs. At the working electrode, a flux boundary is applied, with one flux accounting for CO_2 and the other accounting for CO. The flux of CO_2 (mol/(m^2.s)) is calculated based on the current density resulting from electrolysis at -1.1 V *vs.* RHE in CO_2 and the faradaic efficiencies of all carbon-containing species as follows:

$$Flux = -\frac{j \times FE}{F}$$

$$= -\frac{j}{F} \times \left(\frac{FE_{CO}}{2} + \frac{FE_{CH_4}}{8} + \frac{FE_{C_2H_6}}{7} + \frac{FE_{C_3H_6}}{6} + \frac{FE_{C_3H_8}}{20/3} + \frac{FE_{C_2H_4}}{6} + \frac{FE_{C_4H_{10}}}{6.5} \right)$$

where j (A/m^2) is the electrolysis current density at -1.1V *vs.* RHE in CO_2, F is the Faraday constant (C/mol), and FE is the Faradaic efficiencies of the corresponding products. The Faradaic efficiencies are divided by the number of electrons needed to be injected into one molecule of CO_2 to reduce it to the corresponding species.

Similarly, the flux of CO ($mol/(m^2.s)$) is calculated based on the electrolysis current density at -1.1 V vs. RHE in CO_2 and the faradaic efficiencies of CO:

$$Flux = -\frac{j \times FE_{CO}}{F}$$

where j (A/m^2) is the electrolysis current density at -1.1V *vs.* RHE in CO_2, F is the Faraday constant (C/mol) and FE_{CO} is the Faradaic efficiency of CO.

Similar to the inlet and outlet boundary conditions, inflow and outflow boundary conditions are applied to the bottom-most and top-most boundaries of the tubing, respectively. The concentration of the inflow is set to be the saturated concentration of CO_2 at 25°C (33.4 mM). No flux boundary condition is applied to all other boundaries. Initial values of CO_2 concentration in all domains are set to 33.4 mM and that of CO to be zero.

Table S4 summarizes the parameters used in the two physics modules.

Table S8. Physics parameters used for laminar flow and transport of diluted species physics

Parameters		Value	Unit	Reference
CO_2 diffusion coefficient at 25°C		1.92×10^{-9}	m^2/s	Ager *et al.* [1]
CO diffusion coefficient at 25°C		2.03×10^{-9}	m^2/s	Ager *et al.* [1]
CO_2 saturated concentration in water at 25°C		33.4	mM	Ager *et al.* [1]
Current density at -1.1 V *vs.* RHE		2.52	mA/cm^2	Experimental
Faradaic efficiencies at -1.1 V *vs.* RHE	CO	23.25	%	Experimental
	CH_4	3.81		
	C_2H_6	0.22		
	C_3H_6	0.21		
	C_3H_8	0.11		
	C_2H_4	0.1		
	C_4H_{10}	0.11		
Water viscosity at 25°C		8.90×10^{-4}	Pa/s	COMSOL
Water density at 25°C		997	kg/m^3	COMSOL

Concentration profile throughout the electrochemical cell

The concentration profiles of CO_2 and CO in the electrochemical cell are shown in Fig. S15, which shows the conversion of CO_2 to CO only takes place close to the electrode surface, and the majority of CO_2 passing through the cell is not consumed. This agrees with the gas chromatograph result, as the amount of CO_2 after 2-hour electrolysis at -1.1 V vs. RHE stays relatively unchanged. However, since the electrolyte flow near the corners of the cell is significantly slower, one can observe the decrease of CO_2 and buildup of CO in

these regions, which can exceed the saturated concentration of CO in an aqueous solution.

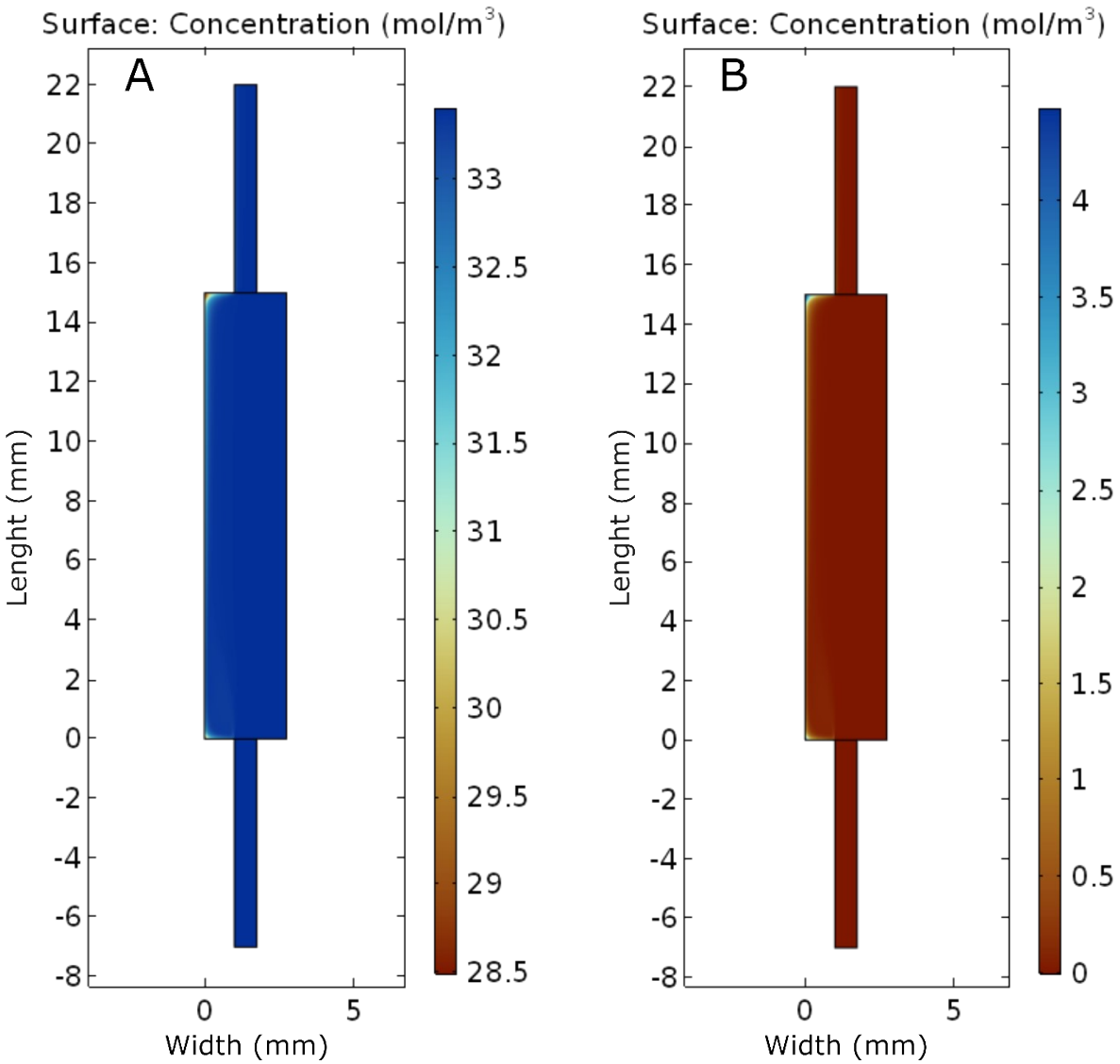

Fig. S15.

Concentration profile in the electrochemical cell of CO_2 (a) and CO (b) when a constant potential of -1.1 V is applied. The x and the y-axis shows the dimension of the cell in mm, and the color graph shows the concentrations.

Concentration profile at specific locations

To better characterize the concentration profile in Fig. S15, the concentrations of CO_2 and CO at the entrance (y = 0), in the middle (y = 7.5 mm), and at the end (y = 15 mm) are plotted as a function of distance from the electrode surface in Fig. S16. The results show significant consumption of CO_2 in the corner of both the entrance and the end, resulting in the increased concentration of CO in these positions above the saturated concentration of CO in an aqueous solution. These concentration patterns are disrupted at 1 mm away from the electrode since the electrolyte is entering and exiting the tubing at this position. In the middle of the electrode, which represents the major surface area of the electrode, the decrease of CO_2 concentration and increase of CO concentration is less pronounced than in the corners. However, in the close vicinity of the electrode (less than 20 μm), CO still exists in a supersaturated state.

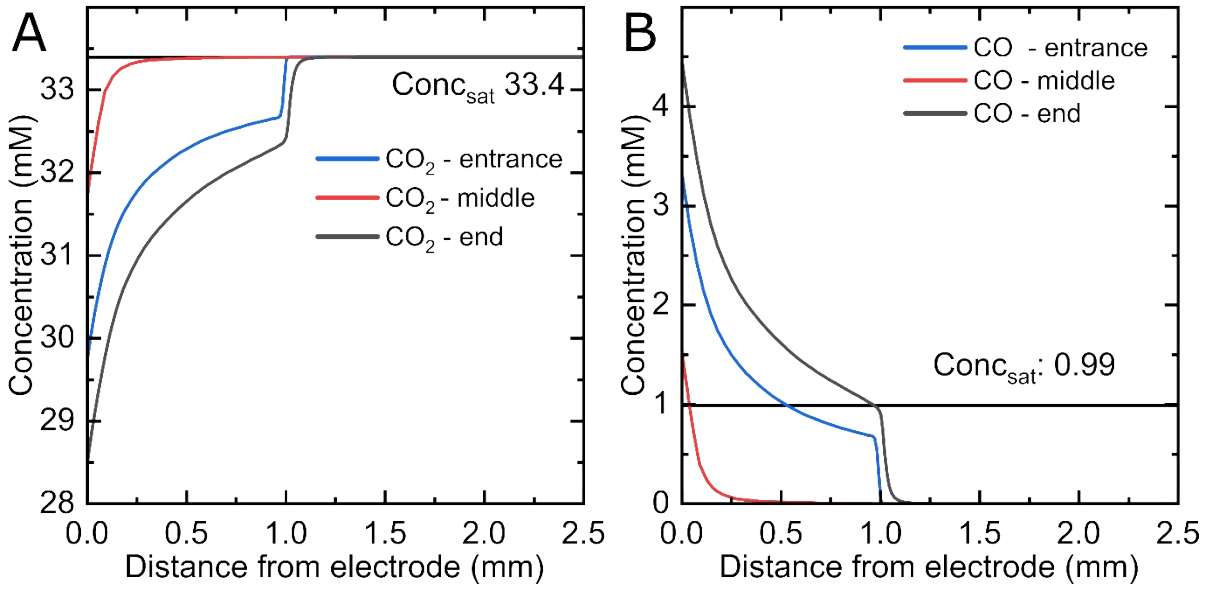

Fig. S16.
Concentration profile as a function of distance from the electrode at the entrance (y = 0), in the middle (y = 7.5 mm), and at the end (y = 15 mm) of the electrochemical cell of CO_2 (a) and CO (b) when a constant potential of -1.1 V vs. RHE is applied.

References

1 Gurudayal, D. Perone, S. Malani, Y. Lum, S. Haussener and J. W. Ager, *ACS Appl. Energy Mater.*, 2019, **2**, 4551–4559.

2 N. O. of D. and Informatics, NIST Chemistry WebBook, https://webbook.nist.gov/chemistry/, (accessed February 24, 2022).

3 P. Roy, M. Rouzières, Z. Qi and O. Chubar, *Infrared Physics & Technology*, 2006, **49**, 139–146.

4 M. Faye, M. Bordessoule, B. Kanouté, J.-B. Brubach, P. Roy and L. Manceron, *Review of Scientific Instruments*, 2016, **87**, 063119.

5 D. Vantelon, N. Trcera, D. Roy, T. Moreno, D. Mailly, S. Guilet, E. Metchalkov, F. Delmotte, B. Lassalle, P. Lagarde and A.-M. Flank, *J Synchrotron Rad*, 2016, **23**, 635–640.

6 B. Ravel and M. Newville, *Phys. Scr.*, 2005, **2005**, 1007.

7 Butane, https://webbook.nist.gov/cgi/cbook.cgi?ID=C106978&Units=SI&Mask=200#Mass-Spec, (accessed February 24, 2022).

8 1-Butene, https://webbook.nist.gov/cgi/cbook.cgi?ID=C106989&Units=SI&Mask=200#Mass-Spec, (accessed February 24, 2022).

9 A. V. Ziminov, S. M. Ramsh, E. I. Terukov, I. N. Trapeznikova, V. V. Shamanin and T. A. Yurre, *Semiconductors*, 2006, **40**, 1131–1136.

10 X. Zhang, Y. Zhang and J. Jiang, *Spectrochimica Acta Part A: Molecular and Biomolecular Spectroscopy*, 2004, **60**, 2195–2200.

11 N. Gupta, M. Gattrell and B. MacDougall, *J Appl Electrochem*, 2006, **36**, 161–172.